



A photometric comparison between the Hyades main sequence and a spectroscopically-chosen sample of field dwarfs

Graeme H. Smith^{1*}

¹University of California Observatories/Lick Observatory, University of California, Santa Cruz, CA 95064, USA

Received 2012 June 23; accepted 2012 August 26

Abstract. A sample of field dwarfs with spectroscopic metallicities derived on a uniform abundance scale by Valenti & Fischer is compared with Hyades main sequence stars in various photometric diagrams. Field dwarfs with metallicities $0.14 \leq [\text{Fe}/\text{H}] \leq 0.29$ are found to match the Hyades ($m_1, b-y$) locus very well. In both the ($M_V, B-V$) colour-magnitude diagram and the ($c_1, b-y$) diagram the Hyades main sequence is found to form a lower envelope to the field dwarfs of this metallicity range. There is no evidence in the comparisons made for the so-called Hyades anomaly.

Keywords : stars: abundances – stars: fundamental parameters (colours)

1. Introduction

The Hyades cluster is ~ 6 Myr old (Perryman et al. 1998; de Bruijne, Hoogerwerf & de Zeeuw 2001; Pinsonneault et al. 2003). At this age, the F and G dwarfs with colours of $(B-V) > 0.3$ should fall close to their zero age main sequence (ZAMS) positions in the colour-magnitude diagram (Castellani, Degl’Innocenti & Prada Moronia 2001). For example, Vandenberg & Poll (1989) found a good match between a model ZAMS computed for ($Y = 0.27, [\text{Fe}/\text{H}] = 0.15$) and the Hyades main sequence in the ($M_V, B-V$) colour-magnitude diagram. Photometric observations of Hyades dwarfs in the Strömgren system have, however, revealed a locus in the gravity-sensitive ($c_1, b-y$) diagram which, when compared to other samples of stars, has led some investigators to infer that the Hyades stars are of lower gravity, and are hence more evolved, than the ZAMS. This phenomenon has been called the ‘Hyades anomaly.’

Comparison between the main sequences of the Coma and Hyades clusters provided the

*e-mail: graeme@ucolick.org

earliest suggestion of this anomaly (Crawford & Barnes 1969). Strömgren, Olsen & Gustafsson (1982) compared the c_1 indices of Hyades F stars to field dwarfs of comparable metallicity. Specifically, field dwarfs in the colour range $0.21 \leq (b - y) \leq 0.41$ were selected so as to have m_1 indices within ± 0.01 mag of the Hyades main sequence at a given $(b - y)$. This corresponds to metallicities within ± 0.11 - 0.14 dex of the Hyades according to the calibration of Nissen (1981). Strömgren et al. (1982) found that in a plot of c_1 versus $(b - y)$ a lower envelope to the field dwarfs was systematically below the Hyades main sequence by ~ 0.03 - 0.04 mag in the c_1 index. This result was not consistent with the Hyades dwarfs defining a zero age main sequence.

Various proposals have been made as to the origin of the Hyades anomaly, including differences in helium abundance (Strömgren et al. 1982), enhanced stellar activity in Hyades stars which causes brightening in some of the bandpasses used to form the c_1 index (Campbell 1984; Rose 1984; Labonte & Rose 1985), and systematic offsets between different c_1 data sets (Eggen 1994). All of these explanations have met with difficulty (e.g. Soderblom 1989; Raddick, Skiff & Lockwood 1990; Dobson 1990; Jøner & Taylor 1995). Barry (1974) compiled empirical evidence that the Hyades anomaly could be explained by a metallicity dependence in both the $b - y$ and c_1 indices due to line blanketing in the spectra of mid-F through early G dwarfs. Nissen (1988) found, however, that the mean c_1 offset between the main sequence of the Hyades and several other open clusters did not correlate with metallicity.

Since the Strömgren et al. (1982) paper the number of dwarf stars for which spectroscopic abundances have become available has increased greatly. In particular, the work of Valenti & Fischer (2005; VF05) has produced homogeneous metallicities for a large sample of dwarfs. In this paper a comparison is presented between Hyades main sequence stars and a subset of the most metal-rich field dwarfs from the Valenti & Fischer (2005) survey. The two samples are compared in the c_1 versus $(b - y)$ diagram to revisit the evidence for anomalous behaviour among the Hyades cluster dwarfs.

2. The stellar samples

A sample of Hyades main sequence stars was chosen from the catalogues of van Bueren (1952), van Altena (1966), and the Leiden survey of Pels, Oort & Pels-Kluyver (1975). Cluster member information was taken from Soderblom (1989), Perryman et al. (1998), de Bruijne et al. (2001), and the WEBDA open cluster database (Mermilliod 1995). In order to obtain a sample that includes as few binaries or multiple systems as possible, stars were excluded if they were listed as binaries or multiples by Stern, Schmitt & Kahabka (1995), Perryman et al. (1998), Böhm-Vitense et al. (2002), or in the WEBDA Hyades database. The online version¹ of the General Catalogue of Photometric Data (Mermilliod, Mermilliod & Hauck 1997; GCPD) was used to obtain Johnson UBV and Strömgren colours for the resulting selection of Hyades dwarfs. The list of Hyades stars and the photometry is given in Table 1 in Appendix 1.

¹Accessed through the World Wide Web at <http://obswww.unige.ch/gcpd/gcpd.html>.

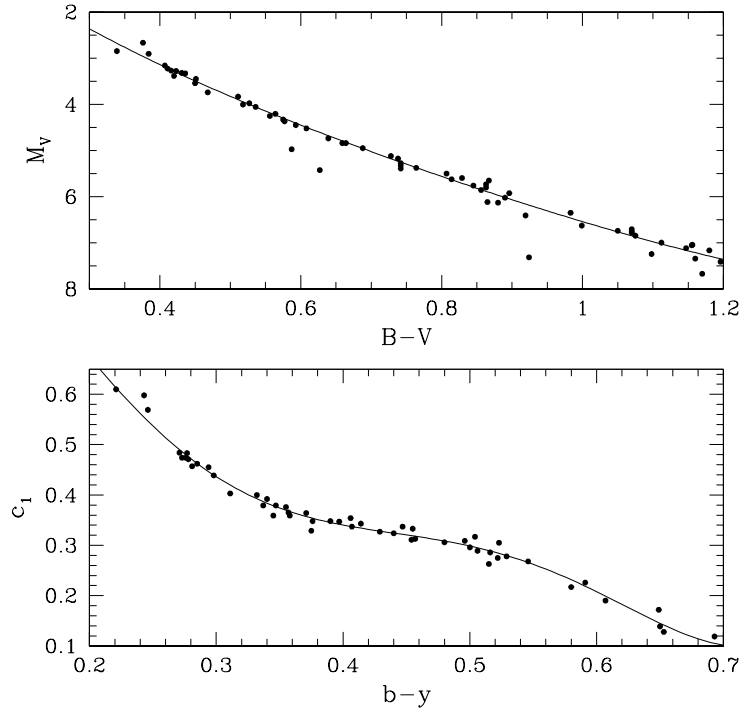


Figure 1. The colour-magnitude diagram (top panel) and locus of c_1 versus $(b-y)$ (bottom panel) of Hyades dwarfs not known to be binaries. Solid lines in the top and bottom panels show the polynomial fits given by equations (1) and (2) respectively.

The work of Valenti & Fischer (2005) has produced a homogeneous catalogue of metallicities for over one thousand dwarf stars of spectral types F, G, and K. These stars were drawn from large extrasolar-planet search programs carried out at Keck Observatory, Lick Observatory, and the Anglo-Australian Telescope (Cumming, Marcy & Butler 1999; Vogt et al. 2000; Tinney et al. 2002; Marcy et al. 2004, 2005). High signal-to-noise spectra of the stars were subjected by VF05 to a uniform abundance analysis. Stars have been selected from the VF05 survey on the basis of metallicity for comparison with Hyades dwarfs. Only field dwarfs with surface gravities of $\log g \geq 4.0$ are considered here, in an effort to reduce the amount of evolution away from the zero age main sequence. Valenti & Fischer (2005) measured abundances for the heavy elements Na, Si, Ti, Fe, and Ni; throughout this paper their $[\text{Fe}/\text{H}]$ values are used for the purposes of dividing stars into metallicity subgroups. Johnson BV photometry and parallaxes for the VF05 stars were obtained from the Hipparcos Catalogue (ESA 1997), with Strömgen four-colour photometry being compiled from the GCPD database.

The field stars in the VF05 sample that will be of most interest in our discussion of the

Hyades anomaly in Section 4 are those with metallicities $0.14 \leq [\text{Fe}/\text{H}] \leq 0.29$ and colours $0.31 \leq (b - y) \leq 0.40$. Such stars fall within the colour range over which Strömgren et al. (1982) documented the anomaly. Photometric data for the relevant VF05 stars are tabulated in Table 2, which includes data in both the Strömgren and Johnson photometric systems as well as the $[\text{Fe}/\text{H}]$ abundance from VF05. The $(b - y)$ and c_1 colours from the GCPD are often mean values derived from multiple observations by multiple sources. In such cases the GCPD also provides values for the observational uncertainties, and where available these are listed as $\epsilon(b - y)$ and $\epsilon(c_1)$ in Table 2. Uncertainties in the $[\text{Fe}/\text{H}]$ abundances as assessed by VF05 are ± 0.05 dex (see Fig. 9 of their paper).

3. Colour-magnitude and two-colour diagrams

The M_V versus $(B - V)$ diagram for Hyades stars not known to be members of binary systems is shown in the top panel of Fig. 1. The parallaxes of de Bruijne et al. (2001) were used where available; for stars with no Hipparcos data a default parallax of 22.2 mas was adopted. Following Perryman et al. (1998), Crawford (1975), and Taylor (1980) the interstellar reddening of the Hyades stars is taken to be negligible. Also shown in Fig. 1 (top panel) is a polynomial fit having the equation

$$M_V = -0.8269 + 13.57352(B - V) - 12.12361(B - V)^2 + 8.43946(B - V)^3 - 2.52049(B - V)^4, \quad (1)$$

which is based on 72 stars, several of the more discrepant points in Fig. 1 being excluded from the fit. The standard deviation in M_V about this fit is 0.12 mag. Equation (1) was chosen because it provided a good visual match to the data and yielded a standard deviation about the fit that was close to 0.1 mag in absolute magnitude.

The Hyades main sequence in the c_1 versus $(b - y)$ diagram of the Strömgren photometric system is shown in the bottom panel of Fig. 1, where again known binary stars have been excluded. The fitted polynomial shown has the equation

$$c_1 = 0.9397 + 4.48305(b - y) - 57.85196(b - y)^2 + 191.05317(b - y)^3 - 260.30386(b - y)^4 + 126.96565(b - y)^5, \quad (2)$$

and provides a good fit over the colour interval $0.2 \leq (b - y) < 0.7$, but is not appropriate for stars redder than this range. The standard deviation in c_1 about the fit, which is based on 56 stars, is 0.015 mag. Equation (2) was chosen on the basis of being the lowest-order fit about which the standard deviation in c_1 was less than 0.02 mag.

Stars from Valenti & Fischer (2005) with $0.14 \leq [\text{Fe}/\text{H}] \leq 0.29$ and $\log g \geq 4.0$ are compared with Hyades single stars in a plot of m_1 versus $(b - y)$ in the top panel of Fig. 2. Hyades stars are plotted as filled circles whereas the VF05 stars are shown as open circles. The m_1 versus $b - y$ relations for these two sets of stars are in good agreement. Thus the photometry confirms that those stars with VF05 metallicities of $0.14 \leq [\text{Fe}/\text{H}] \leq 0.29$ provide a good match in metallicity to the Hyades cluster.

The bottom panel of Fig. 2 shows the M_V versus $(B - V)$ colour-magnitude diagram for stars from Valenti & Fischer (2005) with surface gravities of $\log g \geq 4.0$ and metallicities in the range $0.14 \leq [\text{Fe}/\text{H}] \leq 0.29$. The Hipparcos Catalogue is used as the source of both the parallaxes and the BV photometry used to derive this diagram. The Hyades single-star main sequence is plotted with filled circles. The symbols used for the VF05 dwarfs in the lower panel of Fig. 2 denote surface gravity, with open circles for stars with $\log g \geq 4.3$ and crosses for $4.0 \leq \log g < 4.3$. A number of the lower surface gravity stars with $\log g < 4.3$ may not be ZAMS analogs, but appear to have evolved somewhat away from the main sequence. The Hyades main sequence forms a reasonable baseline to the VF05 dwarfs with metallicities $[\text{Fe}/\text{H}]$ between 0.14 and 0.29 dex and $\log g > 4.3$. As such, the Hyades main sequence seems to constitute a reasonable ZAMS for the VF05 field dwarfs of comparable metallicity.

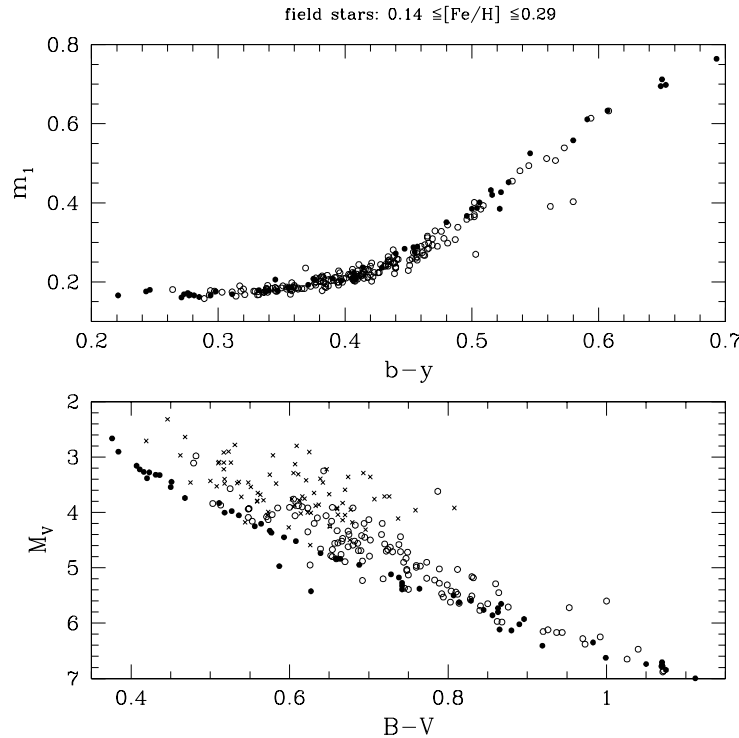


Figure 2. Top panel: The m_1 index versus $(b - y)$ colour for stars from Valenti & Fischer (2005) with metallicities $0.14 \leq [\text{Fe}/\text{H}] \leq 0.29$ and surface gravities $\log g \geq 4.0$ (open circles). Filled circles correspond to non-binary Hyades dwarfs. Bottom panel: The colour-magnitude diagram for stars from Valenti & Fischer (2005) with metallicities $0.14 \leq [\text{Fe}/\text{H}] \leq 0.29$. Open circles show stars having $\log g \geq 4.3$, while crosses correspond to $4.0 \leq \log g < 4.3$. Filled circles denote Hyades dwarfs.

A counterpart to the colour-magnitude diagram is a plot of the gravity index c_1 versus $(b - y)$ colour. It is with such a diagram that Strömgren et al. (1982) identified their version of the Hyades

anomaly, namely the existence of field dwarfs below the locus of the Hyades main sequence, despite the fact that the field stars were chosen to fall within ± 0.01 mag of the Hyades in a $(m_1, b - y)$ diagram. The same stars represented in Fig. 2 are shown in a plot of c_1 versus $(b - y)$ in the top panel of Fig. 3. Open circles are used to designate the VF05 dwarfs with surface gravities of $\log g > 4.0$, while Hyades dwarfs are again shown as filled circles. There is very little trace of a Hyades anomaly in the top panel of Fig. 3, with only ~ 5 stars falling below the locus of the Hyades main sequence. Thus, stars selected from the VF05 survey to have abundances slightly higher than the Hyades cluster fall above the Hyades main sequence in the $(c_1, b - y)$ diagram.

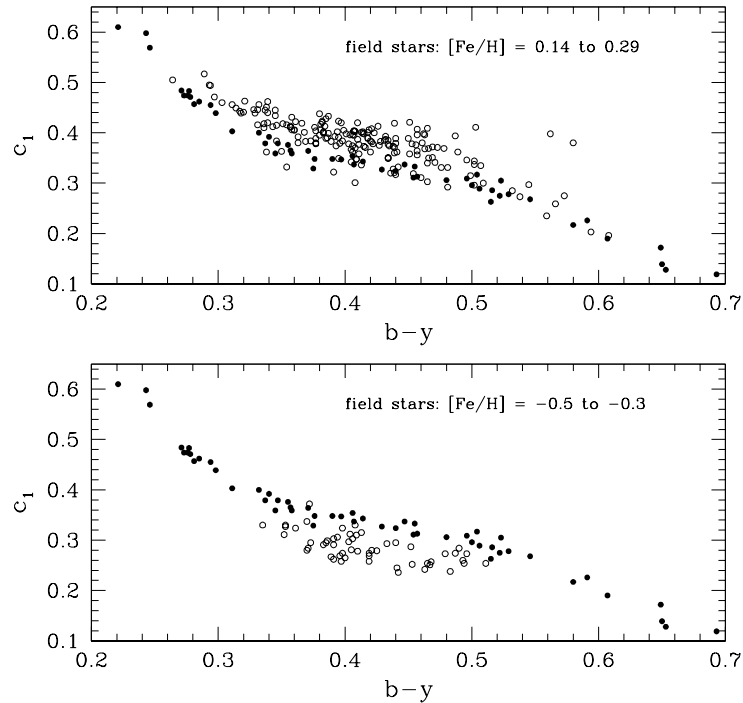


Figure 3. Top panel: The $(c_1, b - y)$ diagram for stars from Valenti & Fischer (2005) with metallicities $0.14 \leq [\text{Fe}/\text{H}] \leq 0.29$. Open circles show VF05 stars with surface gravities of $\log g \geq 4.0$. Filled circles correspond to Hyades non-binary dwarfs. Bottom panel: The $(c_1, b - y)$ diagram for stars from Valenti & Fischer (2005) with metallicities $-0.50 \leq [\text{Fe}/\text{H}] \leq -0.30$. Open circles show VF05 stars with surface gravities of $\log g \geq 4.2$. Filled circles correspond to Hyades non-binary dwarfs.

Stars in the VF05 survey having below-solar metallicities occupy a different region of the $(c_1, b - y)$ diagram than the Hyades cluster. Those stars from VF05 that have metallicities $-0.50 \leq [\text{Fe}/\text{H}] \leq -0.30$ and surface gravities $\log g \geq 4.2$ are shown in the bottom panel of Fig. 3, where they predominantly fall below the Hyades main sequence in the $(c_1, b - y)$ diagram even for colours of $(b - y) \leq 0.4$ (which overlaps the range of the Strömberg et al. 1982 field sample).

Fig. 3 shows a progressive change in the position of dwarfs of different metallicity with respect to the Hyades main sequence in the $(c_1, b - y)$ diagram.

The sample of stars selected by Strömgren et al. (1982) encompassed the colour range $0.2 \leq (b - y) \leq 0.4$, i.e., spectral types from F1V to G2V (see Table II of Bessell 1979), and the anomalous position of the Hyades main sequence relative to the field dwarfs was present throughout this colour range. The field stars employed in this paper by comparison have colours of $0.3 \leq (b - y) \leq 0.6$, i.e., spectral types from F6V to K4V. Hence we are not sampling the same colour range as Strömgren et al. (1982) although there is overlap. Our sample contains G and K dwarfs of later spectral types than in the Strömgren et al. (1982) work, and we lack the F2V-F5V stars that they included.

4. Discussion

The group of field stars in the colour range $0.30 \leq (b - y) \leq 0.41$ that falls below the Hyades main sequence in the $(c_1, b - y)$ diagram of Strömgren et al. (1982) is evidently not represented in the spectroscopic sample of near-Hyades-abundance stars assembled for this paper. One way to account for this would be to postulate that the “below-Hyades” field stars in the study of Strömgren et al. (1982) have lower metal abundances than the Hyades cluster. A comparison of the top and bottom panels of Fig. 3 shows that field dwarfs of different metallicity in the VF05 sample do occupy different locations within the $(c_1, b - y)$ diagram. Whereas the VF05 field sample in Fig. 2 and the top panel of Fig. 3 is restricted to stars with $[\text{Fe}/\text{H}]$ greater than or equal to the Hyades cluster, the field selection criterion used by Strömgren et al. (1982), i.e., stars having m_1 indices within ± 0.01 mag of the Hyades sequence, would allow dwarfs with $[\text{Fe}/\text{H}]$ up to ≈ 0.14 dex below that of the Hyades into their sample. Alternatively it is possible that stars in the VF05 sample are in more evolved phases of evolution than the “below-Hyades” field stars in the study of Strömgren et al. (1982). These possibilities are discussed next.

4.1 Evolution away from the main sequence

For each star in the VF05 sample we denote δc_1 to be the difference between the observed c_1 index and the fiducial Hyades sequence at the $(b - y)$ colour of that star (given by equation 2). Similarly at the $(B - V)$ colour of each star a difference δM_V is determined between the stellar absolute magnitude and that given by the Hyades fiducial locus (equation 1). The δc_1 index is a widely used indicator of absolute magnitude for F dwarfs (e.g., Bell 1971, Eggen 1971, Crawford 1975). We verify this for the F dwarfs in the VF05 sample by Fig. 4, in which δc_1 is plotted versus δM_V for stars with $0.31 \leq (b - y) \leq 0.40$, $\log g \geq 4.0$, and $0.14 \leq [\text{Fe}/\text{H}] \leq 0.20$. There is a clear correlation, and the range in δc_1 values is much larger than the typical observational uncertainties $\epsilon(c_1)$ listed in Table 2.

The range in δc_1 and δM_V residuals observed among the VF05 stars in Fig. 4 can be compared with theoretical models of the zero age main sequence. The difference ΔM_V at a given $(B - V)$

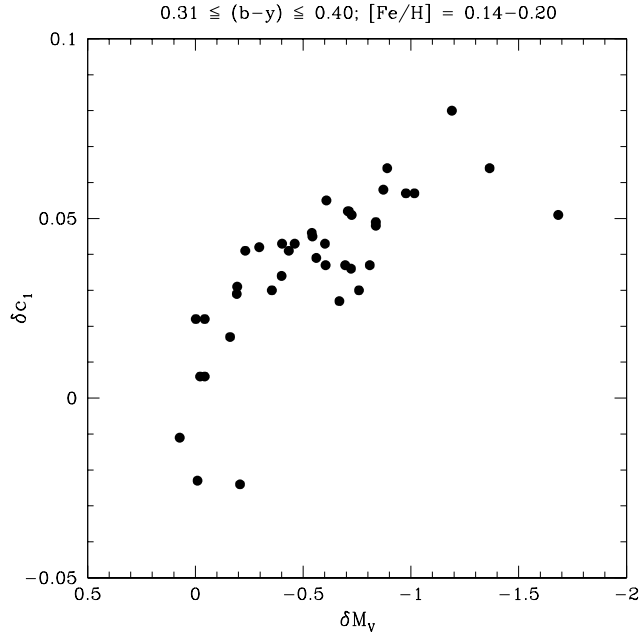


Figure 4. The differential index δc_1 versus magnitude above the fiducial Hyades main sequence δM_V for stars in the survey of Valenti & Fischer (2005) that have $0.31 \leq (b-y) \leq 0.40$, $\log g \geq 4.0$, and $0.14 \leq [\text{Fe}/\text{H}] \leq 0.20$.

colour between a solar metallicity ZAMS and one for a different $[\text{Fe}/\text{H}]$ but the same helium abundance can be calculated from equation (5) of Vandenberg & Poll (1989). Their relation, which is applicable for stars of similar colour to the Sun, indicates that a solar abundance ZAMS should fall $\Delta M_V = 0.21$ mag below the Hyades ZAMS (assuming $[\text{Fe}/\text{H}] = 0.14$ for the Hyades and an identical He abundance to the Sun), whereas a ZAMS for $[\text{Fe}/\text{H}] = 0.28$ would lie 0.22 mag above the Hyades. By contrast, the VF05 sample plotted in Fig. 4 exhibits a range of ≈ 1.5 mag in δM_V and a dispersion in $[\text{Fe}/\text{H}]$ of 0.06 dex. The spread in δM_V and δc_1 indices among these stars cannot be explained by the theoretical dependence of the ZAMS on metallicity. Instead it is inferred that a considerable fraction of the VF05 stars in Fig. 4 are displaced as much as 1.5 mag from their ZAMS positions.

The origin of these displacements can be illustrated with the stellar isochrones of Vandenberg (1985). We consider the grid of isochrones from that paper having $[\text{Fe}/\text{H}] = 0$, $Y = 0.25$, and $\alpha = 1.6$. The absolute magnitude of the ZAMS for this abundance combination is $M_V(\text{ZAMS}) = +4.68$ at a colour of $(B-V) = 0.54$.² An isochrone of a given age is double-valued in absolute

²A solar abundance isochrone from Bell (1988) has colours of $(b-y) = 0.355$ and $(B-V) \sim 0.54$ at an effective temperature of 6000 K. These colours are typical of the region of the main sequence in which the Hyades anomaly is present.

magnitude at this fiducial colour. The fainter of the two points on the isochrone will correspond to relatively low-mass stars that have not yet evolved far from the main sequence. The brighter point on the isochrone will correspond to higher-mass stars that are in more progressed stages of hydrogen burning. Such stars are evolving through the fiducial colour of $(B - V) = 0.54$ during the early stages of their evolution into subgiants. The magnitude of this brighter point is displaced by more than 1.4 mag from the ZAMS at $(B - V) = 0.54$ for stars younger than 6 Gyr. By comparison, the VF05 sample plotted in Figs. 2 and 4 exhibits a spread of up to 1.5 mag in M_V at a colour of $(B - V) \sim 0.54$. This would be expected if the stars had a range in age of ~ 5 Gyr and a range of masses such that some had evolved significantly away from the main sequence.

4.2 Correlation of the c_1 colour with metallicity

Although δc_1 is strongly correlated with δM_V among the VF05 F dwarfs, there is nonetheless evidence for a correlation between δc_1 and stellar metallicity. A plot of δc_1 versus $[\text{Fe}/\text{H}]$ is shown in Fig. 5 for those VF05 field dwarfs that have $0.31 \leq (b - y) \leq 0.40$, $\log g \geq 4.0$, and $0.14 \leq [\text{Fe}/\text{H}] \leq 0.29$. There is certainly scatter but nonetheless a correlation can be discerned, such that an increase in $[\text{Fe}/\text{H}]$ by 0.15 dex above the metallicity of the Hyades may be accompanied by an increase in the value of c_1 by ≈ 0.03 - 0.05 mag. The range in both δc_1 and $[\text{Fe}/\text{H}]$ within Fig. 5 is much larger than the random observational uncertainties in either quantity. On the basis of the correlation seen in Fig. 5, a dwarf with a colour of $(b - y) = 0.31$ to 0.40 and a metallicity 0.14 dex less than the Hyades cluster could be situated 0.03-0.05 mag below the Hyades main sequence in the $(c_1, b - y)$ diagram. This is enough to explain the 0.03 mag by which the Hyades main sequence lies above the baseline for the field stars plotted by Strömgren et al. (1982) in the $(c_1, b - y)$ diagram. Based on the empirical correlation in Fig. 5, those stars in the field sample of Strömgren et al. (1982) that fall below the Hyades main sequence may be more metal-poor than the Hyades.

Twarog, Anthony-Twarog & Tanner (2002) and Twarog, Vargas & Anthony-Twarog (2007) discussed in detail the problems of a metal dependency to the c_1 index. Their work has shown clearly that the c_1 index is very sensitive to metallicity among G dwarfs. The stars in the analysis of Twarog et al. (2007) extend to colours as blue as $(b - y) \sim 0.30$. In the colour range $0.300 \leq (b - y) \leq 0.329$ they find that the c_1 index shows only a weak dependence on metallicity, but that it is very strongly correlated with $[\text{Fe}/\text{H}]$ for $(b - y) > 0.44$, such that for G dwarfs it can be used as a metallicity indicator. The ‘‘Hyades anomaly’’ as delineated by Strömgren et al. (1982) is present throughout the colour range $0.21 \leq (b - y) \leq 0.41$, within which the work of Twarog et al. (2002, 2007) indicates that the metallicity sensitivity of the c_1 index is not as apparent as among the G dwarfs. The question is whether c_1 retains sufficient sensitivity to metallicity to account for the anomaly among F dwarfs.

For dwarfs from the VF05 sample with $0.300 \leq (b - y) \leq 0.329$ Twarog et al. (2007) calibrated the Strömgren m_1 colour versus $[\text{Fe}/\text{H}]$. They found that $d[\text{Fe}/\text{H}]/dm_1 = 10.2$ satisfied the data quite well, with a correlation between m_1 and c_1 across this colour range. Strömgren et al. (1982) restricted their large photometrically-selected sample of field dwarfs to stars that had

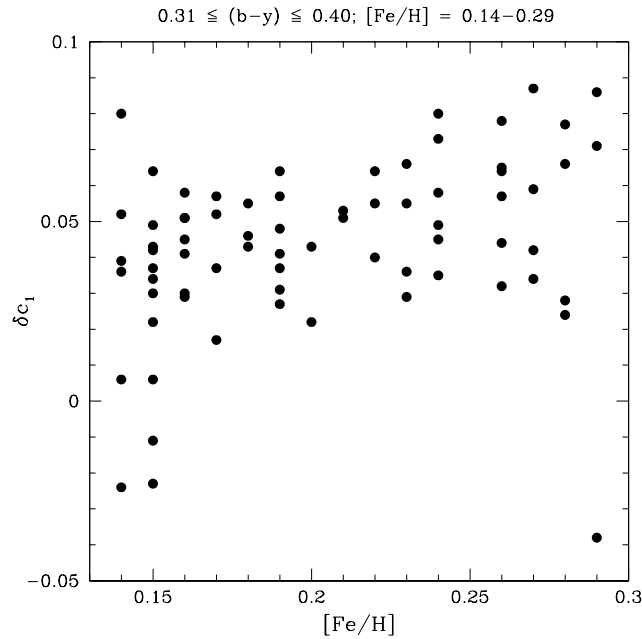


Figure 5. The differential index δc_1 versus iron abundance for stars in the survey of Valenti & Fischer (2005) that have $0.31 \leq (b-y) \leq 0.40$, $\log g \geq 4.0$, and $0.14 \leq [\text{Fe}/\text{H}] \leq 0.29$.

m_1 indices within ± 0.01 mag of the Hyades main sequence. This would imply on the basis of the Twarog et al. (2007) fitting function that Strömgen et al. (1982) were selecting their field dwarfs to have metallicities within ± 0.10 dex of the Hyades cluster. According to Fig. 5 the inclusion of field stars 0.10 dex more metal-poor than the Hyades could have caused some such stars to sit ~ 0.03 mag below the Hyades in the $(c_1, b-y)$ diagram.

Fig. 5 of Twarog et al. (2007) shows that in the $(b-y)$ colour range from 0.300 to 0.329 at metallicities above solar abundance and $m_1 > 0.16$ there is a considerable scatter in $[\text{Fe}/\text{H}]$ at a given m_1 . In fact at $m_1 \sim 0.17$ a spread of 0.3 dex is seen in $[\text{Fe}/\text{H}]$. If this spread is intrinsic rather than due to observational errors in the VF05 measurements of $[\text{Fe}/\text{H}]$, then the selection criterion used by Strömgen et al. (1982) could have included stars more than 0.1 dex different in metallicity from the Hyades cluster, making it more likely that some of their field stars would sit below the Hyades main sequence in $(c_1, b-y)$ diagram.

4.3 Conclusion

The preceding discussion suggests that metallicity effects may be implicated in the form of the Hyades anomaly documented by Strömgen et al. (1982). The criterion used for selecting their

field star sample, namely m_1 indices within ± 0.01 mag of the Hyades main sequence in the $(m_1, b - y)$ diagram, would have led to a sample of field dwarfs within which roughly half of the stars were lower in metallicity than the Hyades cluster. The metallicity differences introduced in this way may not have been large, perhaps on the order of 0.10-0.30 dex depending on how tightly metallicity is correlated with m_1 throughout the $(b - y)$ colour range from 0.20 to 0.40. Nonetheless an unaccounted for correlation between c_1 and $[\text{Fe}/\text{H}]$, coupled with scatter in the intrinsic relation between m_1 and $[\text{Fe}/\text{H}]$, could potentially have led to stars being included in their field sample that had c_1 indices 0.02-0.03 mag less than Hyades dwarfs in the $(c_1, b - y)$ diagram.

The arguments presented above for a metallicity component to the Hyades anomaly fall in the realm of being suggestive but not yet compelling. Some calibrations of Strömgren colours versus stellar parameters, such as that of Meléndez et al. (2010), would indicate that the metallicity sensitivity of the c_1 index is not sufficient to explain the anomaly. Model atmosphere calculations by VandenBerg & Bell (1985) indicate that the Strömgren c_1 index should be sensitive to metallicity for F stars but not to the extent seen in Fig. 5. Furthermore, the sample of field stars with spectroscopic abundances used here is different from the photometrically-selected field sample of Strömgren et al. (1982). As noted in Section 2, stars analysed by Valenti & Fischer (2005) were selected as part of several large exoplanet search efforts. Stars included in such searches may be pre-selected to have low levels of chromospheric activity and intrinsic velocity jitter (Fischer et al. 1999). Chromospheric jitter can become a problem in exoplanet searches via the Doppler technique for dwarfs younger than 3 Gyr (Marcy & Butler 1998). As such dwarfs located close to the zero age main sequence might be selected against in the VF05 sample. What is needed is the addition of field dwarfs with spectroscopic metallicities on the VF05 abundance scale that are $\sim 1 - 2$ Gyr old in order to determine whether these also fall above the Hyades main sequence in the $(c_1, b - y)$ diagram.

Acknowledgements

This research has made use of the WEBDA database, operated at the Institute for Astronomy of the University of Vienna, as well as the online version of The General Catalogue of Photometric Data maintained by J. -C. Mermilliod, B. Hauck, & M. Mermilliod.

References

- Barry D. C., 1974, *AJ*, 79, 616
- Bell R. A., 1971, *MNRAS*, 155, 65
- Bell R. A., 1988, *AJ*, 95, 1484
- Bessell M. S., 1979, *PASP*, 91, 589
- Böhm-Vitense E., Robinson R., Carpenter K., Mena-Werth J., 2002, *ApJ*, 569, 941
- Campbell B., 1984, *ApJ*, 283, 209
- Castellani V., Degl'Innocenti S., Prada Moronia P. G., 2001, *MNRAS*, 320, 66
- Crawford D. L., Barnes J. V., 1969, *AJ*, 74, 407

- Crawford D. L., 1975, *AJ*, 80, 955
- Cumming A., Marcy G. W., Butler R. P. 1999, *ApJ*, 526, 890
- de Bruijne J. H. J., Hoogerwerf R., de Zeeuw P. T., 2001, *A&A*, 367, 111
- Dobson A. K., 1990, *PASP*, 102, 88
- Eggen O. J., 1971, *PASP*, 83, 741
- Eggen O. J., 1994, *AJ*, 107, 594
- ESA, 1997, *The Hipparcos and Tycho Catalogues*, ESA SP-1200
- Fischer D. A., Marcy G. W., Butler R. P., Vogt S. S., Apps K., 1999, *PASP*, 111, 50
- Joner M. D., Taylor B. J., 1995, *PASP*, 107, 124
- Labonte B. J., Rose J. A., 1985, *PASP*, 97, 790
- Marcy G. W., Butler R. P., 1998 *ARA&A*, 36, 57
- Marcy G. W., Butler R. P., Fischer D. A., Vogt S. S., 2004, in Beaulieu J.-P., Lecavelier des Etangs A., Terquem C., eds, *Extrasolar Planets: Today and Tomorrow*, ASP Conf. Ser. 321, Astronomical Society of the Pacific, San Francisco, p. 3
- Marcy G. W., Butler R. P., Vogt S. S., Fischer D. A., Henry G. W., Laughlin G., Wright J. T., Johnson J. A., 2005, *ApJ*, 619, 570
- Meléndez J., Schuster W. J., Silva J. S., Ramírez I., Casagrande L., Coelho P., 2010, *A&A*, 522, A98
- Mermilliod J. -C. 1995, in Egret D. & Albrecht M. A., eds, *Information and On-Line Data in Astronomy*, Kluwer Academic Press, Dordrecht, p. 127
- Mermilliod J. -C., Mermilliod M., Hauck B., 1997, *A&AS*, 124, 349
- Nissen P. E., 1981, *A&A*, 97, 145
- Nissen P. E., 1988, *A&A*, 199, 146
- Pels G., Oort J. H., Pels-Kluyver H. A., 1975, *A&A*, 43, 423
- Perryman M. A. C., et al., 1998, *A&A*, 331, 81
- Pinsonneault M. H., Terndrup D. M., Hanson R. B., Stauffer J. R., 2003, *ApJ*, 598, 588
- Raddick R. R., Skiff B. A., Lockwood G. W., 1990, *ApJ*, 353, 524
- Rose J. A., 1984, *AJ*, 89, 1238
- Soderblom D. R., 1989, *ApJ*, 342, 823
- Stern R. A., Schmitt J. H. M. M., Kahabka P. T., 1995, *ApJ*, 448, 683
- Strömgren B., Olsen E. H., Gustafsson B., 1982, *PASP*, 94, 5
- Taylor B. J., 1980, *AJ*, 85, 242
- Tinney C. G., Butler R. P., Marcy G. W., Jones H. R. A., Penny A. J., McCarthy C., Carter B. D., 2002, *ApJ*, 571, 528
- Twarog B. A., Anthony-Twarog B. J., Tanner D., 2002, *AJ*, 123, 2715
- Twarog B. A., Vargas L. C., Anthony-Twarog B. J., 2007, *AJ*, 134, 1777
- van Altena W. F., 1966, *AJ*, 71, 482
- van Bueren H. G., 1952, *Bull. Astr. Inst. Netherlands*, 11, 385
- Valenti J. A., Fischer D. A., 2005, *ApJS*, 159, 141
- VandenBerg D. A., 1985, *ApJS*, 58, 711
- VandenBerg D. A., Bell R. A., 1985, *ApJS*, 58, 561
- VandenBerg D. A., Poll H. E., 1989, *AJ*, 98, 1451
- Vogt S. S., Marcy G. W., Butler R. P., Apps K. 2000, *ApJ*, 536, 902

A. Appendix 1

The Hyades cluster stars considered in this paper are listed in Table 1 together with photometric data compiled from the literature sources noted in Section 2. Star designations used in Table 1 are vB for van Bueren (1952), vA for van Altena (1966), and Pe for Pels et al. (1975).

Table 1: Photometry of Hyades Stars.

Star	$(b - y)$	m_1	c_1	$(B - V)$	$(U - B)$	V	M_V
vB004	0.845	0.538	8.886	5.76
vB006	0.221	0.166	0.610	0.339	-0.001	5.972	2.85
vB007	0.523	0.427	0.305	0.896	0.631	8.986	5.93
vB010	0.375	0.208	0.329	0.593	0.100	7.850	4.45
vB013	0.278	0.168	0.471	0.420	-0.010	6.620	3.38
vB015	0.407	0.223	0.337	0.659	0.202	8.086	4.84
vB016	0.273	0.169	0.474	0.423	0.005	7.051	3.28
vB018	0.406	0.210	0.354	0.639	0.168	8.060	4.74
vB019	0.332	0.179	0.400	0.511	0.029	7.116	3.83
vB021	0.480	0.351	0.306	0.814	0.468	9.146	5.62
vB025	0.546	0.525	0.268	0.983	0.805	9.596	6.35
vB026	0.455	0.276	0.333	0.742	0.331	8.626	5.32
vB027	0.440	0.272	0.324	0.728	0.307	8.445	5.12
vB031	0.357	0.186	0.365	0.564	0.067	7.473	4.21
vB035	0.285	0.162	0.462	0.436	-0.013	6.800	3.33
vB037	0.271	0.161	0.484	0.407	0.000	6.610	3.16
vB044	0.298	0.176	0.439	0.450	0.028	7.186	3.54
vB046	0.500	0.385	0.296	0.863	0.541	9.117	5.73
vB048	0.337	0.176	0.379	0.518	0.039	7.135	4.00
vB049	0.376	0.206	0.348	0.587	0.122	8.240	4.97
vB051	0.294	0.166	0.455	0.451	-0.002	6.958	3.45
vB053	0.243	0.176	0.598	0.376	0.032	5.988	2.67
vB064	0.414	0.237	0.343	0.664	0.201	8.109	4.84
vB065	0.347	0.177	0.379	0.536	0.057	7.420	4.05
vB066	0.358	0.186	0.359	0.556	0.054	7.506	4.25
vB073	0.390	0.209	0.348	0.608	0.127	7.846	4.52
vB074	0.114	0.225	0.912	0.220	0.120	5.025	1.67
vB076	0.764	0.394	9.190	5.38
vB086	0.311	0.169	0.403	0.468	0.000	7.039	3.74
vB087	0.457	0.289	0.313	0.742	0.351	8.588	5.27
vB090	0.276	0.172	0.474	0.416	-0.008	6.380	3.27
vB092	0.454	0.288	0.311	0.742	0.339	8.657	5.39
vB093	0.516	0.420	0.286	0.880	0.576	9.399	6.13
vB094	0.281	0.166	0.457	0.431	-0.007	6.620	3.32
vB097	0.397	0.203	0.347	0.627	0.074	8.711	5.42

Table 1. (continued)

Star	$(b - y)$	m_1	c_1	$(B - V)$	$(U - B)$	V	M_V
vB099	0.506	0.401	0.289	0.865	0.598	9.382	6.11
vB100	0.246	0.180	0.569	0.384	0.008	6.038	2.90
vB105	0.345	0.206	0.359	0.577	0.097	7.530	4.37
vB109	0.807	0.448	9.401	5.50
vB110	0.429	0.236	0.327	0.688	0.245	8.854	4.95
vB116	0.496	0.367	0.309	0.829	0.511	8.993	5.60
vB118	0.371	0.193	0.364	0.575	0.101	7.740	4.33
vB127	0.447	0.284	0.337	0.738	0.347	8.890	5.18
vB129	0.080	0.203	1.031	0.155	0.142	4.637	1.04
vB143	0.340	0.178	0.392	0.527	0.059	7.896	3.98
vB153	0.856	0.563	8.916	5.86
vB154	0.277	0.166	0.483	0.411	0.000	5.802	3.22
vB173	0.693	0.764	0.119	1.232	1.180	10.500	7.49
vB174	0.591	0.611	0.226	1.050	0.956	9.993	6.74
vB180	0.504	0.387	0.317	0.863	0.564	9.083	5.80
vB181	0.649	0.695	0.172	1.155	1.079	10.320	7.05
vB183	0.529	0.452	0.278	0.919	0.680	9.675	6.41
vB191	0.740	0.786	0.139	1.298	1.200	11.034	7.66
vA075	1.29	1.08	10.97	7.66
vA171	0.924	...	9.810	7.32
vA294	0.730	0.804	0.069	1.289	1.283	10.892	7.66
vA407	0.653	0.698	0.128	1.147	1.020	10.474	7.12
vA500	1.289	1.152	10.692	7.42
vA548	1.156	1.092	10.312	7.04
vA684	0.522	0.385	0.275	0.867	0.481	8.92	5.65
Pe008	1.07	...	10.12	6.78
Pe010	0.515	0.432	0.263	0.890	0.580	9.30	6.02
Pe011	1.070	1.030	10.142	6.75
Pe015	1.180	1.120	10.487	7.17
Pe016	0.580	0.558	0.217	0.999	0.890	9.938	6.63
Pe026	1.224	1.220	10.830	7.56
Pe064	1.098	1.030	10.511	7.24
Pe065	1.196	1.170	10.738	7.41
Pe066	1.239	1.163	10.672	7.50
Pe080	0.607	0.633	0.190	1.075	1.000	10.042	6.85
Pe093	1.112	1.060	10.684	7.00
Pe096	0.650	0.712	0.139	1.160	...	10.610	7.34
Pe098	1.07	...	10.29	6.70
Pe101	1.170	1.160	10.937	7.67
Pe119	1.277	1.270	10.915	7.63

B. Appendix 2

Photometry for field stars from Valenti & Fischer (2005) with colours $0.31 \leq (b - y) \leq 0.40$ and metallicities $0.14 \leq [\text{Fe}/\text{H}] \leq 0.29$ is listed in Table 2. Sources of the data are discussed in Section 2. The observational uncertainties in the $(b - y)$ and c_1 colours are denoted $\epsilon(b - y)$ and $\epsilon(c_1)$ respectively.

Table 2: Photometry of Field Stars from Valenti and Fischer (2005).

HD	V	M_V	$(B - V)$	$[\text{Fe}/\text{H}]$	c_1	$\epsilon(c_1)$	$(b - y)$	$\epsilon(b - y)$	δM_V	δc_1
377	7.59	4.59	0.626	0.15	0.322	0.006	0.391	0.002	-0.010	-0.023
5470	8.36	4.20	0.631	0.24	0.393	0.392	-0.428	0.049
6558	8.20	3.86	0.606	0.26	0.411	0.003	0.376	0.001	-0.623	0.057
7570	4.97	4.08	0.571	0.16	0.392	0.007	0.363	0.004	-0.192	0.029
8673	6.34	3.43	0.500	0.15	0.449	0.314	-0.400	0.034
8941	6.60	3.10	0.526	0.19	0.456	0.007	0.332	0.004	-0.890	0.064
9562	5.75	3.39	0.639	0.26	0.405	0.010	0.399	0.004	-1.289	0.064
9826	4.10	3.45	0.536	0.15	0.415	0.006	0.346	0.002	-0.604	0.037
19994	5.07	3.32	0.575	0.19	0.422	0.003	0.361	0.001	-0.977	0.057
21313	8.18	3.92	0.623	0.19	0.380	0.377	-0.668	0.027
21847	7.29	3.84	0.503	0.20	0.416	0.331	-0.002	0.022
24112	7.24	3.65	0.560	0.14	0.406	0.001	0.358	0.006	-0.561	0.039
30339	8.21	3.88	0.611	0.26	0.395	0.380	-0.635	0.044
30562	5.77	3.65	0.631	0.26	0.420	0.008	0.397	0.003	-0.978	0.078
31253	7.13	3.48	0.583	0.16	0.419	0.005	0.366	0.003	-0.872	0.058
35850	6.30	4.16	0.553	0.29	0.332	0.020	0.354	0.002	-0.007	-0.038
40979	6.74	4.13	0.573	0.17	0.380	0.004	0.363	0.002	-0.161	0.017
42024	7.24	3.54	0.551	0.18	0.434	0.005	0.345	0.001	-0.608	0.055
52265	6.29	4.05	0.572	0.19	0.406	0.005	0.360	0.002	-0.231	0.041
52447	8.38	3.90	0.605	0.24	0.423	0.003	0.382	0.000	-0.576	0.073
53665	7.26	3.22	0.517	0.17	0.446	0.001	0.331	0.004	-0.712	0.052
63754	6.54	2.97	0.579	0.22	0.431	0.358	-1.348	0.064
67556	7.30	3.94	0.548	0.19	0.412	0.000	0.343	0.001	-0.194	0.031
70110	6.18	3.13	0.607	0.15	0.413	0.004	0.384	0.002	-1.365	0.064
70843	7.06	3.72	0.539	0.16	0.418	0.005	0.336	0.002	-0.355	0.030
71479	7.17	4.06	0.646	0.21	0.402	0.383	-0.657	0.053
72780	7.47	3.87	0.513	0.15	0.410	0.000	0.336	0.001	-0.043	0.022
74868	6.56	3.78	0.567	0.24	0.418	0.001	0.351	0.000	-0.472	0.045
75289	6.35	4.04	0.578	0.22	0.405	0.360	-0.274	0.040
75332	6.22	3.93	0.549	0.14	0.362	0.000	0.338	0.003	-0.207	-0.024
75782	7.09	2.80	0.609	0.29	0.421	0.005	0.382	0.007	-1.701	0.071
82082	7.20	3.76	0.605	0.14	0.389	0.015	0.377	0.004	-0.722	0.036
82943	6.54	4.35	0.623	0.27	0.390	0.386	-0.238	0.042
84737	5.08	3.75	0.619	0.17	0.383	0.003	0.389	0.001	-0.809	0.037

Table 2. (continued)

HD	V	M_V	$(B - V)$	[Fe/H]	c_1	$\epsilon(c_1)$	$(b - y)$	$\epsilon(b - y)$	δM_V	δc_1
86264	7.41	3.11	0.510	0.26	0.443	0.317	-0.785	0.032
89744	5.73	2.78	0.531	0.26	0.451	0.001	0.338	0.002	-1.250	0.065
102634	6.15	3.48	0.518	0.18	0.439	0.005	0.329	0.003	-0.461	0.043
102870	3.59	3.40	0.518	0.18	0.416	0.009	0.354	0.003	-0.540	0.046
105328	6.72	3.80	0.613	0.16	0.400	0.383	-0.725	0.051
106423	7.50	3.90	0.616	0.29	0.433	0.387	-0.641	0.086
107213	6.38	2.90	0.523	0.28	0.462	0.008	0.339	0.004	-1.076	0.077
107692	6.70	4.66	0.639	0.15	0.349	0.395	-0.022	0.006
115383	5.19	3.92	0.585	0.28	0.384	0.004	0.373	0.003	-0.439	0.028
120136	4.50	3.53	0.508	0.23	0.439	0.002	0.318	0.003	-0.343	0.029
124115	6.42	3.11	0.479	0.23	0.456	0.000	0.311	0.001	-0.578	0.036
130087	7.52	3.78	0.612	0.28	0.417	0.004	0.381	0.001	-0.740	0.066
131117	6.30	3.29	0.605	0.14	0.428	0.014	0.385	0.004	-1.190	0.080
133161	7.01	4.27	0.599	0.21	0.400	0.002	0.383	0.001	-0.175	0.051
139324	7.49	3.88	0.633	0.15	0.374	0.393	-0.759	0.030
147723	5.40	2.91	0.625	0.16	0.404	0.377	-1.683	0.051
150933	7.19	3.99	0.573	0.15	0.401	0.001	0.368	0.000	-0.296	0.042
157968	6.20	2.92	0.517	0.17	0.463	0.004	0.321	0.006	-1.016	0.057
159063	6.98	3.47	0.534	0.22	0.440	0.007	0.339	0.001	-0.576	0.055
163272	7.39	4.02	0.614	0.23	0.406	0.381	-0.515	0.055
165269	7.29	3.31	0.611	0.27	0.438	0.380	-1.206	0.087
169586	6.75	3.46	0.548	0.23	0.445	0.345	-0.676	0.066
169830	5.90	3.10	0.517	0.15	0.446	0.009	0.328	0.002	-0.837	0.049
179949	6.25	4.09	0.548	0.14	0.384	0.004	0.346	0.004	-0.043	0.006
185720	6.97	3.57	0.525	0.24	0.445	0.003	0.337	0.000	-0.421	0.058
187691	5.12	3.68	0.563	0.16	0.413	0.005	0.357	0.002	-0.543	0.045
192343	8.01	3.92	0.680	0.28	0.383	0.369	-0.994	0.024
193795	8.50	4.23	0.683	0.19	0.379	0.001	0.396	0.005	-0.695	0.037
196800	7.21	4.06	0.607	0.16	0.389	0.009	0.385	0.003	-0.433	0.041
196885	6.39	3.80	0.559	0.20	0.411	0.006	0.357	0.009	-0.402	0.043
199190	6.86	4.01	0.627	0.15	0.384	0.003	0.398	0.002	-0.601	0.043
201203	7.89	3.09	0.511	0.27	0.441	0.320	-0.811	0.034
206332	7.41	3.91	0.600	0.27	0.402	0.004	0.394	0.002	-0.539	0.059
206395	6.67	3.79	0.559	0.24	0.420	0.339	-0.409	0.035
213240	6.81	3.76	0.603	0.14	0.399	0.002	0.387	0.006	-0.707	0.052
216435	6.03	3.42	0.621	0.24	0.423	0.015	0.395	0.001	-1.155	0.080
218261	6.44	4.18	0.544	0.15	0.363	0.002	0.350	0.005	0.073	-0.011
222033	7.21	3.71	0.616	0.19	0.391	0.000	0.395	0.002	-0.837	0.048